International Journal of Obesity (2015), 1–8

www.nature.com/ijo

ORIGINAL ARTICLE

G_{M3} ganglioside and phosphatidylethanolamine-containing lipids are adipose tissue markers of insulin resistance in obese women

JM Wentworth[1,2], G Naselli[1], K Ngui[1], GK Smyth[3,4], R Liu[3], PE O'Brien[2], C Bruce[5], J Weir[6], M Cinel[6], PJ Meikle[6,7] and LC Harrison[1,7]

AIMS: The association between central obesity and insulin resistance reflects the properties of visceral adipose tissue. Our aim was to gain further insight into this association by analysing the lipid composition of subcutaneous and omental adipose tissue in obese women with and without insulin resistance.

METHODS: Subcutaneous and omental adipose tissue and serum were obtained from 29 obese non-diabetic women, 13 of whom were hyperinsulinemic. Histology, lipid and gene profiling were performed.

RESULTS: In omental adipose tissue of obese, insulin-resistant women, adipocyte hypertrophy and macrophage infiltration were accompanied by an increase in G_{M3} ganglioside and its synthesis enzyme ST3GAL5; in addition, phosphatidylethanolamine (PE) lipids were increased and their degradation enzyme, phosphatidylethanolamine methyl transferase (PEMT), decreased. *ST3GAL5* was expressed predominantly in adipose stromovascular cells and *PEMT* in adipocytes. Insulin resistance was also associated with an increase in PE lipids in serum.

INTERPRETATION: The relevance of these findings to insulin resistance in humans is supported by published mouse studies, in which adipocyte G_{M3} ganglioside, increased by the inflammatory cytokine tumour necrosis factor-α, impaired insulin action and PEMT was required for adipocyte lipid storage. Thus in visceral adipose tissue of obese humans, an increase in G_{M3} ganglioside secondary to inflammation may contribute to insulin resistance and a decrease in PEMT may be a compensatory response to adipocyte hypertrophy.

International Journal of Obesity accepted article preview 26 October 2015; doi:10.1038/ijo.2015.223

INTRODUCTION

Central obesity is strongly associated with insulin resistance[1,2] and type 2 diabetes.[3] It is characterized by an increase in circulating free fatty acids and inflammatory markers, and a decrease in circulating adiponectin, perturbations that lead to insulin resistance in liver and muscle.[4,5] These changes are likely to result from dysfunction of hypertrophied adipocytes because adipose tissue from obese people, particularly visceral adipose tissue, has impaired insulin sensitivity[6,7] and releases more fatty acids[8] and inflammatory cytokines[9,10] and less adiponectin.[9,10]

Adipose tissue of insulin-resistant people is enriched for saturated fatty acids and ceramide,[11,12] lipids that induce insulin resistance by different mechanisms: saturated fatty acids induce insulin resistance through pro-inflammatory toll-like receptor 4 signalling pathways[13] and inflammasome activation,[14] and ceramide impairs insulin receptor signalling by inhibiting a key downstream mediator, protein kinase B.[15] In addition, the ceramide derivative G_{M3} ganglioside interacts with and inhibits insulin receptor signalling.[16] In rodents, blocking ceramide or G_{M3} ganglioside synthesis ameliorates diet-induced insulin resistance.[17–19]

The advent of high-throughput mass spectrometry has enabled comprehensive lipid profiling of human tissues. Studies comparing omental and subcutaneous adipose tissue from obese people reported enrichment of ceramide[20] and differential expression of multiple mostly glycerolipid species in omental fat,[21] but provided no interpretation of these findings. To identify lipid signatures and clues to the mechanisms of insulin resistance, we performed comprehensive lipidomic profiling of omental and subcutaneous adipose tissue from obese women with and without insulin resistance. Gene expression analysis was then performed to identify enzymatic determinants of the lipid profile associated with insulin resistance.

MATERIALS AND METHODS

Subjects and tissue

Tissue donors were non-diabetic (defined as fasting glucose < 7 mmol l^{-1} and HbA1c $< 6.5\%$), obese women without liver disease or levels of serum alanine and aspartate transaminases > 50 IU l^{-1} who were undergoing elective gastric band surgery. Participants were not on low-calorie diets during the 2 months before surgery and none were taking fibrates, metformin or other insulin sensitisers. Three women (one in the IS Group and two IR Group) were taking statins. Donors gave written, informed consent and the study was approved by The Human Research Ethics Committees of the Walter and Eliza Hall Institute and the Avenue Hospital, Melbourne. Biochemical analytes were measured by Melbourne Pathology (Abbottsford, VIC, Australia) within the preceding two months. HOMA-IR, a measure of insulin resistance, was estimated as (insulin (mU l^{-1}))x(glucose

[1]Molecular Medicine Division, Walter and Eliza Hall Institute of Medical Research, Parkville, Victoria, Australia; [2]Monash University Centre for Obesity Research and Education, Melbourne, Victoria, Australia; [3]Bioinformatics Division, Walter and Eliza Hall Institute of Medical Research, Parkville, Victoria, Australia; [4]Department of Mathematics and Statistics, University of Melbourne, Carlton, Victoria, Australia; [5]Centre for Physical Activity and Nutrition Research, School of Exercise and Nutrition Sciences, Deakin University, Melbourne, Victoria, Australia and [6]Baker IDI Heart and Diabetes Institute, Melbourne, Victoria, Australia. Correspondence: Dr JM Wentworth Molecular Medicine Division Walter and Eliza Hall Institute of Medical Research, 1G Royal Parade, Parkville, Victoria 3055, Australia.
E-mail: wentworth@wehi.edu.au
[7]Joint senior authors.
Received 13 April 2015; revised 10 September 2015; accepted 13 October 2015

(mmol l^{-1}))/22.5. On the day of surgery, blood was obtained before anaesthesia and the serum stored for later measurement of adiponectin by ELISA (R&D Systems, MN, USA). Visceral and subcutaneous adipose tissue specimens were resected from the omentum near the angle of His and from the periumbilical region, respectively. They were placed in DME medium (Sigma, Sydney, NSW, Australia) at room temperature and processed within 3 h of surgery.

Lipidomic analyses

Adipose tissue (20–100 mg) was pulverised under liquid nitrogen, re-suspended in 300 µl phosphate-buffered saline, placed at 4 °C overnight and then sonicated for 15 s (30 J). Aliquots of 50 µl were combined with 60 µl of phosphate-buffered saline, re-sonicated, dried by vacuum for 14 h and re-suspended in 20 µl water. Internal standards were added and lipid extracted using 2:1 chloroform:methanol in a single phase. Serum lipids were extracted as previously described.[22] Samples were reconstituted in 50 µl water-saturated butanol and 50 µl methanol supplemented with 10 mM ammonium formate and analysed on an Agilent 1200 UPLC coupled to an AB Sciex 4000 Q/TRAP mass spectrophotometer and Analyst v1.5 software (Applied Biosystems, Melbourne, VIC, Australia), as previously described.[22] Each adipose tissue lipid species and lipid class/subclass (sum of the individual species within a class/subclass) was expressed relative to phosphatidylcholine (PC), the predominant cell membrane lipid. Duplicate adipose tissue samples from two donors were used to determine that the intra-assay coefficients of variation (CVs). CVs for phospholipids and sphingolipids were $<13\%$, and for glycerolipids and cholesterol were 26 and 19%, respectively.

RNA preparation and PCR with reverse transcription

RNA was prepared from pulverised adipose tissue using Tri Reagent (Invitrogen). Total RNA was reverse-transcribed with Superscript III (Invitrogen) and amplified on an ABI Prism 7700 platform using the Sybergreen reporter (Qiagen, Valencia, CA, USA). Primer pairs (Supplementary Table 1) were shown to have comparable amplification efficiency across a 1000-fold range of cDNA concentrations, with gene expression relative to β-actin determined using the comparative CT method.

Gene microarray analysis

RNA was hybridised to Illumina HumanHT-12 BeadChips at the Australian Genome Research Facility. Data were exported from Illumina's GenomeStudio software and analysed using the limma package. Intensity values were normexp background corrected and quantile normalised using the neqc function of limma.[23] Probes were filtered as non-expressed if they failed to achieve a detection *P*-value of 0.1 on at least six arrays. Differential expression was assessed using empirical Bayes moderated *t*-tests.[24] For genes within the specified GO categories, *P*-values were adjusted to control the false discovery rate at $<5\%$.

Histology

Adipose tissue processing, sectioning and staining has been described previously.[25] Digital images were obtained using an Aperio scanner and representative 5x images captured using Imagescope v11.1 software (Vista, CA, USA). Image analysis (ImageJ, Bethesda, MD, USA) was performed in a blinded manner. For each section, between 300 and 2000 adipocytes >100 µm^2 were identified to determine mean adipocyte area (*A*), which was converted to diameter with the formula $D=2\times(A/\pi)^{0.5}$.

Adipose tissue digestion

Adipose tissue (~3 g) was digested in 10 ml DME medium supplemented with 10 mg ml^{-1} fatty acid-depleted BSA (Calbiochem, San Diego, CA, USA), 35 µg ml^{-1} Liberase blendzyme 3 (Roche, Indianapolis, IN, USA) and 60 units ml^{-1} DNAse I (Sigma) at 37 °C as previously described.[25] Adipocytes and adipose stromovascular cells were washed in phosphate-buffered saline and either lysed in Tri Reagent for subsequent RNA extraction.

Statistical analysis

Analysis was performed with Prism version 5.0a software for Macintosh (Graphpad, San Diego, CA, USA). Groups were compared by the Mann–Whitney test or Wilcoxon matched-pairs test, as appropriate. To control for multiple comparisons of concentrations of different lipids between groups we used the method of Benjamini and Hochberg with a false discovery rate $<5\%$. Multiple groups were analysed by analysis of variance, with Newman–Keuls post-test comparisons of group pairs. Correlations were determined by Spearman's rank correlation coefficient.

RESULTS

Characteristics of obese women discordant for insulin resistance

To determine whether insulin resistance in obesity was associated with specific lipid species in adipose tissue, we identified non-diabetic obese women with ($n=13$; IR Group) and without ($n=16$; 'insulin-sensitive' or IS Group) fasting hyperinsulinaemia (Table 1). Average age, body mass index, fasting glucose and liver enzyme concentrations were similar between the groups. When compared to IS women, IR women had higher concentrations of triglyceride and lower concentrations of high-density lipoprotein cholesterol and adiponectin, and were more likely to have albuminuria.

Omental adipocyte size and macrophage density correlate with insulin resistance

Adipocyte cross sectional area was determined by morphological analysis of formalin-fixed adipose tissue. IR women were characterized by omental adipocyte hypertrophy, and the degree of systemic insulin resistance (HOMA-IR) correlated with omental but not subcutaneous adipocyte size (Figure 1a). We then determined the relationship between adipose tissue inflammation and insulin resistance. Expression of CD68mRNA, a marker of adipose tissue macrophage density,[26] was highest in IR omental tissue (Figure 1b), and correlated with HOMA-IR ($R=0.41$, $P<0.05$; Figure 1c). In addition, the concentration of tumour necrosis factor-alpha mRNA in omental adipose tissue correlated significantly with HOMA-IR ($R=0.39$, $P<0.05$). Thus, in obese women, we confirmed as shown previously by ourselves[25] and others,[7]

Table 1. Characteristics of IS and IR women

	IS (n = *16*)	*IR* (n = *13*)
Clinical		
Age	46.7 (8.7)	45.6 (11.4)
Weight (kg)	110.3 (12.9)	121.7 (24.4)
Height (cm)	158 (5.4)	163 (5.2)*
Body mass index (kg m^{-2})	44.1 (5.0)	45.6 (7.8)
Waist circumference (cm)	120 (9.4)	127 (13.4)
Waist/hip ratio	0.87 (0.07)	0.89 (0.04)
Hypertension (n)	5 (31%)	5 (38%)
Albuminuria (n)[a]	0	4 (31%)*
Biochemical[b]		
Fasting plasma glucose (mmol l^{-1})	5.3 (0.5)	5.5 (0.5)
Fasting insulin (mU l^{-1})	7.7 (1.8)	29.3 (7.2)***
HOMA-R (mmol mU l^{-2} per 22.5)	1.8 (0.5)	7.1 (2.0)***
Fasting C-peptide (pmol l^{-1})	741 (180)	1615 (304)***
HbA1c (%)	5.6 (0.2)	5.7 (0.2)
HbA1c (mmol mol^{-1})	38 (2)	39 (2)
Fasting triglyceride (mmol l^{-1})	1.3 (0.4)	2.1 (1.4)*
Total cholesterol (mmol l^{-1})	5.5 (0.8)	5.3 (0.7)
HDL cholesterol (mmol l^{-1})	1.6 (0.2)	1.3 (0.3)**
Alanine transaminase (U l^{-1})	22 (9.4)	27 (8.4)
Aspartate transaminase (U l^{-1})	18 (4.9)	21 (4.5)
γ-Glutamyl transferase (U l^{-1})	25 (20.6)	32 (9.9)
Adiponectin (mg l^{-1})[c]	11.7 (4.6)	5.6 (3.5)**

Abbreviations: HDL, high-density lipoprotein; IR, insulin-resistant; IS, insulin-sensitive. Continuous variables are mean (s.d.). *, ** and ***$P<0.05$, $P<0.01$ and $P<0.001$, respectively [a]defined as albumin/creatinine ratio >3.5 mg-mmol^{-1}. [b]Performed on fasting blood collected in the 2 months before surgery. [c]Two IS and one IR serum sample not available for this analysis.

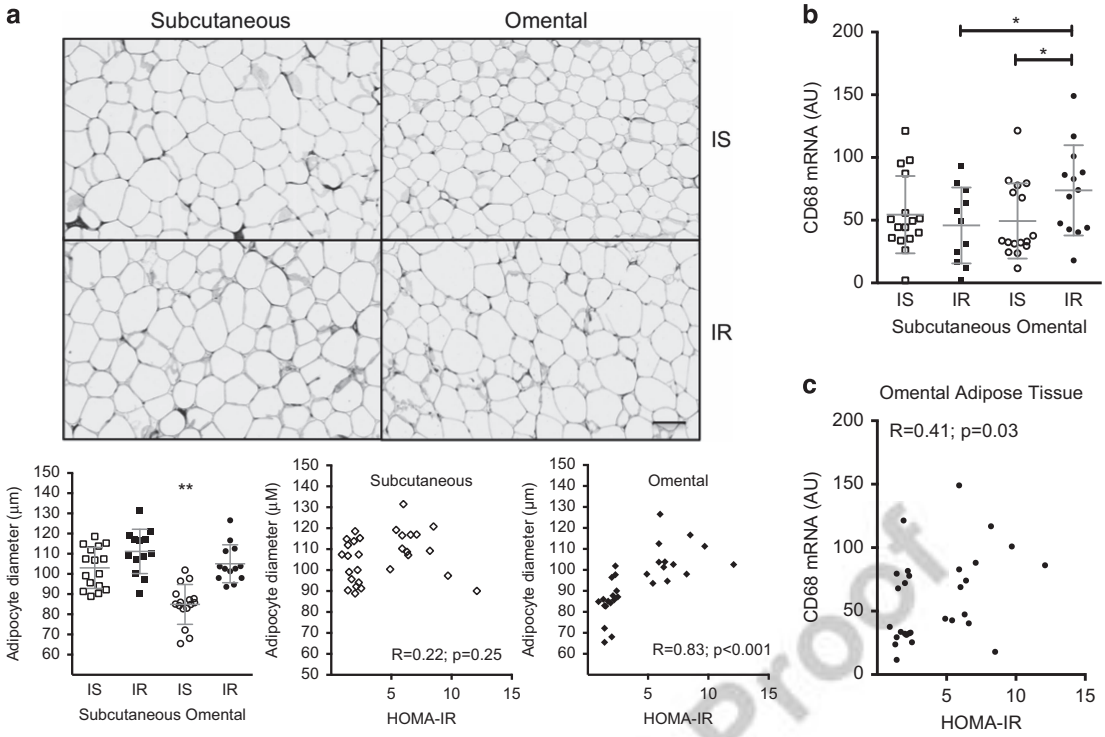

Figure 1. Insulin resistance in obesity is characterized by adipocyte hypertrophy and increased $CD68^+$ macrophage infiltration into omental adipose tissue. (**a**) Representative adipose tissue sections of subcutaneous and omental adipose tissue from IS and IR women (scale bar, 100 μm), and analyses of mean adipocyte diameter according to subject group and adipose tissue depot, and insulin resistance (HOMA-IR). (**b**) *CD68* expression according to subject group and adipose tissue depot. (**c**) Association between omental CD68 mRNA expression and HOMA-IR. * and ** $P < 0.05$ and $P < 0.01$.

that insulin resistance is associated with omental adipocyte hypertrophy and increased macrophage infiltration into omental adipose tissue.

Insulin resistance is associated with specific sphingolipids and phospholipids in omental adipose tissue

A schematic overview of the sphingo- and phospholipids described below along with their relevant metabolism enzymes is provided in Figure 2. To determine if insulin resistance was associated with differences in lipid species, we compared the lipidomic profiles of subcutaneous and omental adipose tissue from IS and IR women (Table 2). Lipid concentrations were normalised to the abundant membrane lipid, PC. After correcting for multiple comparisons, insulin resistance was associated with changes in only one class of lipid, dihexosylceramide, the concentration of which was higher in omental adipose tissue of IS compared with IR women. An analysis of the 265 individual lipid species showed none was differentially abundant in IS and IR women after correction for multiple comparisons. Without multiple comparison correction, eight lipid species were differentially present to a statistical significance of $P < 0.01$ (Table 3). Each species was from the omental depot and two were dihexosylceramide species.

Because hypertrophy and inflammation were most marked in omental adipose tissue of IR women (Figure 1) we compared subcutaneous and omental adipose tissue lipid concentrations to determine if there were a lipid profile of hypertrophy and inflammation. This revealed clear lipid differences, which were magnified in IR women (Table 2). In both IS and IR women, omental adipose tissue had a distinct sphingolipid signature when compared to subcutaneous adipose tissue, characterized by higher concentrations of ceramide and lower concentrations of sphingomyelin and trihexosylceramide. For glycerolipids, alkylphosphatidylcholine (PC[O]), alkenylphosphatidylcholine (PC[P]) and lysophosphatidylcholine were more abundant in subcutaneous than omental adipose tissue in both IS and IR women. However, some lipids were differentially abundant only in IR women: their subcutaneous adipose tissue was enriched for dihexosylceramide and their omental adipose tissue for G_{M3} ganglioside and phosphatidylethanolamine (PE) and its ether derivatives PE[O] and PE[P] (Tables 2 and 3).

Serum lipid analysis identifies phosphatidylinositol and PE lipids as markers of insulin resistance

To identify circulating lipids as potential markers of insulin resistance, we compared the lipid profiles of day-of-surgery serum samples from 14 IS and 12 IR women (Table 4). Triglyceride concentrations in this analysis correlated with those obtained from blood samples obtained in the 2 months prior to surgery ($R = 0.53$; $P < 0.01$). Insulin resistance was associated with higher concentrations of serum phosphatidylinositol and with di- and triglycerides. In addition, concentrations of PE, PE[O] and PE[P], which were selectively enriched in omental adipose tissue of IR women (Table 2), were higher in the sera of IR women and correlated significantly with HOMA-R ($R = 0.63$, $P < 0.001$; $R = 0.46$, $P < 0.02$; and $R = 0.55$, $P < 0.005$ respectively).

Gene expression identifies potential determinants of differential lipid abundance

To identify lipid metabolism enzymes, we performed gene microarray comparison of subcutaneous and omental adipose tissue from six IR women whose lipid profiles mirrored those of the entire IR group (Supplementary Figure and Supplementary Table 2). Focusing on genes assigned the terms 'sphingolipid metabolic process' and/or 'glycerolipid metabolic process' in the

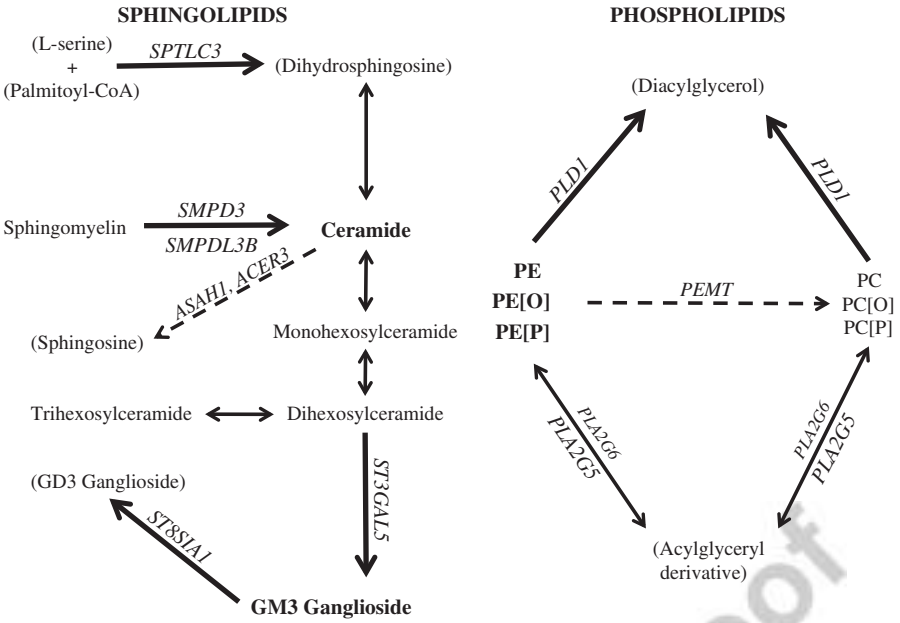

Figure 2. Overview of main findings. Lipids enriched in omental adipose tissue (Table 2) are indicated by a large bold font. The concentrations of bracketed lipids were not determined. The enzymes linking the lipids are indicated in italic capital font. Enzymes whose mRNAs were enriched in omental adipose tissue are indicated by their larger font and increased thickness of the arrow leading from their lipid substrate to its product. Dashed arrows accompany enzymes whose mRNA concentrations were lower in omental compared with subcutaneous adipose tissue.

Table 2. Concentrations of 18 lipid classes in adipose tissue from IS and IR women

Lipid	*IS* (n = *16*)		*IR* (n = *13*)	
	Subcutaneous	*Omental*	*Subcutaneous*	*Omental*
Ceramide	41 (7.5)	81.5 (32.9)***	41.5 (8.3)	90.8 (40.3)***
Monohexosylceramide	4.9 (2.9)	3.4 (1.5)	4.1 (1.1)	4 (1.0)
Dihexosylceramide	5.6 (3.9)	4.7 (1.6)	4.1 (2.1)	2.9 (0.9)* ##
Trihexosylceramide	12.7 (4.4)	6.9 (2.3)***	12.9 (5.5)	7.4 (2.2)**
G_{M3} ganglioside	7.3 (3.0)	7.7 (2.2)	5.9 (2.3)	8.8 (1.1)**
Sphingomyelin	240.6 (32.0)	144.4 (27.8)***	246.8 (44.0)	147.5 (55.0)***
PC[O]	72.7 (13.4)	39.4 (8.7)***	69.1 (16.5)	45.6 (10.8)***
PC[P]	108.1 (26.5)	55.8 (12.4)***	102.3 (20.9)	60.1 (10)***
Lysophosphatidylcholine	34.9 (13.1)	15.9 (3.3)***	32.1 (9.5)	13.7 (3.2)***
PE	146.6 (67.2)	140.3 (25.6)	123.8 (17.3)	151.9 (16.7)**
PE[O]	10.1 (2.9)	11.4 (3.6)	8.7 (3.5)	13.8 (2.2)**
PE[P]	161 (45)	195 (35)	143 (53)	209 (31)*
Lysophosphatidylethanolamine	71.6 (28.9)	70.3 (22.2)	62.6 (18.7)	54.7 (18.4)
Phosphatidylinositol	198.6 (25.7)	182.2 (16)	181.3 (22.9)	185.9 (24.4)
Phosphatidylserine	252.8 (50.3)	219.8 (24.3)	231.6 (34.6)	235.7 (26.4)
Cholesterol (×1000)	40.3 (12.7)	27.8 (15.5)*	33.9 (11)	21.5 (9.5)*
Diglyceride (×1000)	14.2 (2.9)	13.8 (4.5)	12.6 (2.4)	12.8 (2.8)
Triglyceride (×1000)	740 (338.1)	576.7 (321.3)	785.9 (272.8)	585.8 (226.6)

Abbreviations: PC, phosphatidylcholine; PC[O], alkylphosphatidylcholine; PC[P], alkenylphosphatidylcholine; PE, phosphatidylethanolamine; PE[O], alkylphosphatidylethanolamine; PE[P], alkenylphosphatidylethanolamine; IS, insulin-sensitive; IR, insulin-resistant. Data are mean (s.d.) of lipid concentration (mmol mol^{-1} PC). *, ** and *** are corrected $P < 0.05$, $P < 0.01$ and < 0.001 for subcutaneous vs omental within each group. ## is $P < 0.01$ for IS v IR.

Gene Ontology Consortium[27] identified 68 differentially expressed genes. Of these, seven sphingolipid and four PE metabolism genes were listed in sphingolipid and glycerophospholipid pathways defined by the Kyoto Encyclopedia of Genes and Genomes[28] (Table 5). Their differential expression was broadly consistent with the lipid profile of omental adipose tissue. Thus, increased expression of *SPTLC3*, *SMPDL3* and *SMPD3B* (encoding serine palmitoyltransferase subunit 3, and sphingomyelin phosphodiesterase 3 and -3B, respectively) and decreased expression of *ASAH1* and *ACER3* (encoding N-acylsphingosine amidohydrolase 1 and alkaline ceramidase 3, respectively) are consistent with the increase in ceramide and the decrease in sphingomyelin; increased expression of *ST3GAL5* (encoding ST3 beta-galactoside alpha-2, 3-sialyltransferase 5) is consistent with the increase in G_{M3} ganglioside and decreased expression of *PEMT* (phosphatidylethanolamine methyl transferase; encoding phosphatidylethanolamine *N*-methyltransferase) with the increase in PE, PE[O] and PE [P] (Table 2).

The microarray findings were validated by PCR with reverse transcription of adipose tissue RNA from all 29 women. Genes exhibiting greater than twofold differential expression by microarray were documented with the exception of *SMPDL3B*, which

could not be amplified (Figure 3a). Expression of *PEMT* was lower in omental compared with subcutaneous adipose tissue, particularly in IR women. Expression of *SMPD3* was increased in omental compared to subcutaneous adipose tissue, the difference being more marked in IR women. Levels of *ST3GAL5* mRNA were much lower and not significantly different between IS and IR women. However, in the total group, *ST3GAL5* expression was higher in omental than subcutaneous adipose tissue (mean ± s.d. of 2.7 ± 1.6 and 1.7 ± 1.3 respectively; $P = 0.03$).

To determine if expression of *PEMT*, *SMPD3* or *ST3GAL5* corresponded with enzyme activity we compared their respective product/substrate ratios in both adipose tissue depots from each group (Figure 3b). In both groups, the decreased expression of *PEMT* observed in omental fat was reflected in a decreased ratio of PC[O]/PE[O] (Figure 3b), and of PC[P]/PE[P] and lysophosphatidylcholine/lysophosphatidylethanolamine (not shown). Similarly, increased expression of *SMPD3* in omental adipose tissue reflected a higher ceramide/sphingomyelin ratio. The G_{M3} ganglioside/dihexosylceramide ratio was strikingly elevated in IR omental adipose tissue, consistent with increased expression of *ST3GAL5* enriching this depot for G_{M3} ganglioside (Table 2). In each case, the expression of *PEMT*, *SMPD3* or *ST3GAL5* was significantly correlated with their product/substrate ratios (Figure 3c).

Table 3. Lipid species differentially present to a significance of $P < 0.01$ in omental adipose tissue of IS and IR women

Lipid	*IS*	*IR*	P
PE[P-16:0/20:4]	39 (15)	57 (11)	0.0009
Phosphatidylinositol 36:2	19.6 (8.8)	10.7 (3.5)	0.0021
PC[O-35:4]	0.08 (0.07)	0.15 (0.04)	0.0036
Dihexosylceramide 16:0	1.9 (0.8)	1.1 (0.5)	0.0039
Dihexosylceramide 22:0	1.2 (0.4)	0.7 (0.5)	0.0074
PE[18:0/20:3]	5.3 (2.1)	7.1 (1.1)	0.0086
PE[P-18:0/18:2]	30 (12)	20 (5)	0.0095
Phosphatidylserine 38:3	14.8 (3.7)	19.3 (5)	0.0099

Abbreviations: IR, insulin-resistant; IS, insulin-sensitive; PC, phosphatidylcholine; PE, phosphatidylethanolamine. Data are mean (s.d.) of lipid concentration (mmol mol^{-1} PC). *P*-value not corrected for multiple comparisons.

To determine the cell origin of differentially expressed lipid enzymes, we performed PCR with reverse transcription on adipocytes and stromovascular cells (containing endothelial, immune and stem cells) prepared from paired subcutaneous and omental adipose tissues from seven obese non-diabetic IR women. Accurate cell separation was shown by enrichment of leptin and PPAR-γ, and depletion of CD68, mRNA in adipocytes compared to stromovascular cells (Supplementary Table 3). Expression of *PEMT* was higher in adipocytes whereas expression of *SMPD3* and *ST3GAL5* was higher in stromovascular cells (Supplementary Table 3). Compared with subcutaneous tissue, expression of *PEMT* was decreased in omental tissue adipocytes whereas expression of *SMPD3* and *ST3GAL5* in omental stromovascular cells was increased.

DISCUSSION

To gain further insight into the mechanisms of insulin resistance in obesity, we analysed lipids and their synthesis enzymes in subcutaneous and omental adipose tissue from obese women with and without insulin resistance. As previously reported,[7,29] insulin resistance was associated with adipocyte hypertrophy and increased macrophage density in the omental depot. Surprisingly though, the overall lipid profiles of omental adipose tissue from IS and IR women were similar. This is most likely explained by heterogeneity among individuals because differential expression of several lipids was apparent when the lipid profiles of paired subcutaneous and omental tissues were compared. These included PE lipids, dihexosylceramide and G_{M3} ganglioside, which were differentially abundant in IR women. Gene expression analysis then identified PEMT, SMPD3 and ST3GAL5 as the most likely determinants of the omental adipose tissue lipidome in IR women.

Hypertrophic omental adipose tissue in IR women was characterized by a decreased concentration of the ST3GAL5 substrate dihexosylceramide and an increased G_{M3} ganglioside/dihexosylceramide ratio, indicative of increased ST3GAL5 activity. ST3GAL5 and G_{M3} ganglioside have previously been implicated as mediators of insulin resistance. Thus, genetic[30] or pharmacological blockade upstream of ST3GAL5[18,19] protected mice from diet-

Table 4. Lipidomic profile of serum obtained from insulin-sensitive (IS) and insulin-resistant (IR) women immediately prior to gastric band surgery

	IS (n = 14)	*IR (n = 12)*	P
Ceramide	7.3 (2.8)	9.5 (3.5)	0.09
Monohexosylceramide	6.8 (2.6)	8 (4.3)	0.36
Dihexosylceramide	4.5 (1.4)	4.6 (2.1)	0.91
Trihexosylceramide	1.4 (0.4)	1.5 (0.8)	0.68
G_{M3} ganglioside	2.3 (0.8)	2.4 (0.9)	0.77
Sphingomyelin	348.3 (104.1)	380 (103.1)	0.45
PC	764.7 (193.7)	891.8 (227.9)	0.14
PC[O]	21.1 (6.6)	23.2 (7.5)	0.46
PC[P]	12.3 (4.3)	12.9 (4.1)	0.69
Lysophosphatidylcholine	184.4 (49.6)	164.7 (49.1)	0.32
PE	11.5 (5.5)	21.6 (17.5)	0.05
PE[O]	0.9 (0.4)	1.6 (1.2)	0.05
PE[P]	10 (5)	17 (12)	0.04
Lysophosphatidylethanolamine	20.1 (7.3)	22.7 (7.8)	0.39
Phosphatidylinositol	80.5 (26.9)	125.3 (49.2)	0.01
Phosphatidylserine	0.4 (0.2)	0.5 (0.3)	0.44
Cholesterol	815.6 (262)	964.9 (331.9)	0.21
Cholesterol ester	1171.6 (236.3)	1305.7 (265.7)	0.19
Diglyceride	75.5 (26.3)	108.7 (44.6)	0.03
Triglyceride	321.1 (123.9)	539.1 (287.6)	0.02

Abbreviations: PC, phosphatidylcholine; PC[O], alkylphosphatidylcholine; PC[P], alkenylphosphatidylcholine; PE, phosphatidylethanolamine; PE[O], alkylphosphatidylethanolamine; PE[P], alkenylphosphatidylethanolamine; IS, insulin-sensitive; IR, insulin-resistant. Data are mean (s.d.) of lipid concentration (μmol l^{-1}). *P*-value not corrected for multiple comparisons.

Table 5. Lipid metabolism genes differentially expressed in omental versus subcutaneous adipose tissue of IR women

Gene Symbol (Illumina probe ID)	*Gene name*	*Enzymatic function*	*Log_2Fold Change*[a]
Sphingolipid genes			
ASAH1 (2030482)	N-acylsphingosine amidohydrolase	Converts ceramide to sphingosine	−0.57
ACER3 (1230017)	Alkaline ceramidase 3	Converts ceramide to sphingosine	−0.49
SPTLC3 (3780743)	Serine palmitoyltransferase subunit 3	Rate-limiting first step of *de novo* ceramide synthesis	0.60
ST8SIA1 (5360025)	ST8 alpha-*N*-acetyl-neuraminide alpha-2, 8-sialyltransferase 1	Converts G_{M3}- to G_{D3} ganglioside	1.00
ST3GAL5 (5260403)	ST3 beta-galactoside alpha-2, 3-sialyltransferase 5	Converts dihexosylceramide to G_{M3} ganglioside	1.14
SMPDL3B (4390221)	Sphingomyelin phosphodiesterase 3B	Converts sphingomyelin to ceramide	1.24
SMPD3 (4490324)	Sphingomyelin phosphodiesterase 3	Converts sphingomyelin to ceramide	2.01
Glycerolipid genes			
PEMT (1780411)	Phosphatidylethanolamine *N*-methyltransferase	Converts PE, PE[O] and PE[P] to PC, PC[O] and PC[P], respectively	−1.29
PLA2G6 (4640682)	Phospholipase A2, group VI	First step in catabolism of PE, PC and their ether derivatives	−0.50
PLD1 (5050689)	Phospholipase D1	Removes choline from PC, PC[O] and PC[P] and ethanolamine from PE, PE[O] and PE[P]	0.63
PLA2G5 (4480468)	Phospholipase A2, group V	First step in catabolism of PE, PC and their ether derivatives	0.64

Abbreviations: PC, phosphatidylcholine; PC[O], alkylphosphatidylcholine; PC[P], alkenylphosphatidylcholine; PE, phosphatidylethanolamine; PE[O], alkylphosphatidylethanolamine; PE[P], alkenylphosphatidylethanolamine; IR, insulin-resistant. [a]Negative and positive values reflect enrichment in subcutaneous and omental adipose tissue, respectively. PC and PE: phosphatidylcholine and phosphatidylethanolamine, respectively.

induced insulin resistance. Furthermore, TNF-α-induced insulin resistance in mouse adipocytes is mediated by G_{M3} ganglioside,[31] which interacts with a lysine residue proximal to the insulin receptor transmembrane domain and inhibits insulin signalling.[16] Together, our findings are consistent with the idea that, in obesity, adipocyte hypertrophy and inflammation in omental adipose tissue increases ST3GAL5 activity and G_{M3} ganglioside production, leading to impaired insulin action in adipocytes. These changes may represent a compensatory response to limit adipocyte size that would also limit the ability of omental adipose tissue to store lipid, thereby increasing its delivery to the liver to cause hepatic steatosis and systemic insulin resistance.

A recent study identified a locus near *PEMT* associated with abdominal obesity, supporting a role for PEMT in human insulin resistance.[32] Our finding of decreased *PEMT* expression in omental compared to subcutaneous adipose tissue extends previous studies[21,33,34] by identifying a decrease in the PC/PE ratio indicative of decreased PEMT activity. Expression of *PEMT* was higher in adipocytes compared with stromovascular cells, suggesting that adipocytes are the predominant site of PEMT action in adipose tissue. This is consistent with the dramatic upregulation of mRNA for PEMT during differentiation of mouse 3T3 fibroblasts into adipocytes, which require PEMT to generate lipid droplets for storage.[35] The observed decrease in PEMT in hypertrophic omental adipocytes may be another compensatory response to protect adipocytes from lipid overload, leading to adipocyte necrosis and reactive inflammation.[36]

We confirmed that omental adipose tissue is enriched for ceramide[20,37] and mRNA encoding SMPD3.[37] Expression of *SMPD3* was higher in stromovascular cells compared to adipocytes, consistent with localisation of SMPD3 to blood vessels[37] and suggesting that stromovascular cells govern the accumulation of ceramide in omental adipose tissue. Ceramide has been implicated mechanistically in the insulin resistance of obesity as an inhibitor of signalling downstream of the insulin receptor (reviewed in Lipina and Hundal[15]). However, our observations that adipose tissue ceramide concentrations and ceramide/sphingomyelin ratios are similar in IR and IS women suggests that ceramide is not central to insulin resistance in humans and argues against targeting SMPD3 as a therapeutic approach.

The concentration of triglyceride, the most abundant lipid species in adipose tissue,[20] did not differ between adipose tissue depots or between IR and IS women, consistent with previous reports.[20,21] However, as in other studies,[38,39] serum concentrations of triglycerides, diglycerides and ceramide were markers of insulin resistance. Sera of obese IR women were also enriched for phosphatidylinositol, PE, PE[O] and PE[P], whose levels correlated robustly with HOMA-R. We have reported previously the potential of these and other plasma lipids as markers of insulin resistance and type 2 diabetes in both men and women.[40,41]

The findings of this study require several qualifications. First, because we only studied women we cannot assume that PE-lipid enrichment in omental adipose tissue is also a feature of insulin resistance in men. Second, the differential abundance of G_{M3} ganglioside and PE lipids in omental adipose tissue, and the association of these lipids with insulin resistance, do not establish causality. Furthermore, differences in mRNA expression do not necessarily reflect differences in encoded proteins, although the correlation we observed between *PEMT, SMPD3* and *ST3GAL5* mRNA and their respective product/substrate ratios suggests this is in fact the case, and a prior study has confirmed increased SMPD3 protein in omental adipose tissue.[37] Finally, more detailed cellular and sub-cellular localisation of lipids is required to be certain that the observed differences in lipid abundance are all functionally relevant. For example, the increase in G_{M3} ganglioside in IR omental adipose tissue might not be expected to impair insulin action in adipocytes if it were limited to stromovascular cells or even if it occurred in cellular locations other than membrane caveolae.[16]

In summary, comprehensive lipidomic profiling identifies G_{M3} ganglioside and PE lipids, and mRNAs encoding their synthesis enzymes, as markers of insulin resistance in omental adipose tissue in obese women. Previous studies in mice demonstrated that inhibition of G_{M3} ganglioside production protects against diet-induced insulin resistance.[18,19] Our finding in obese insulin-resistant women that G_{M3} ganglioside is increased in omental adipose tissue suggests therefore that G_{M3} ganglioside mediates insulin resistance in humans. Drugs that target the G_{M3} pathway may therefore have therapeutic value for insulin resistance in obesity.

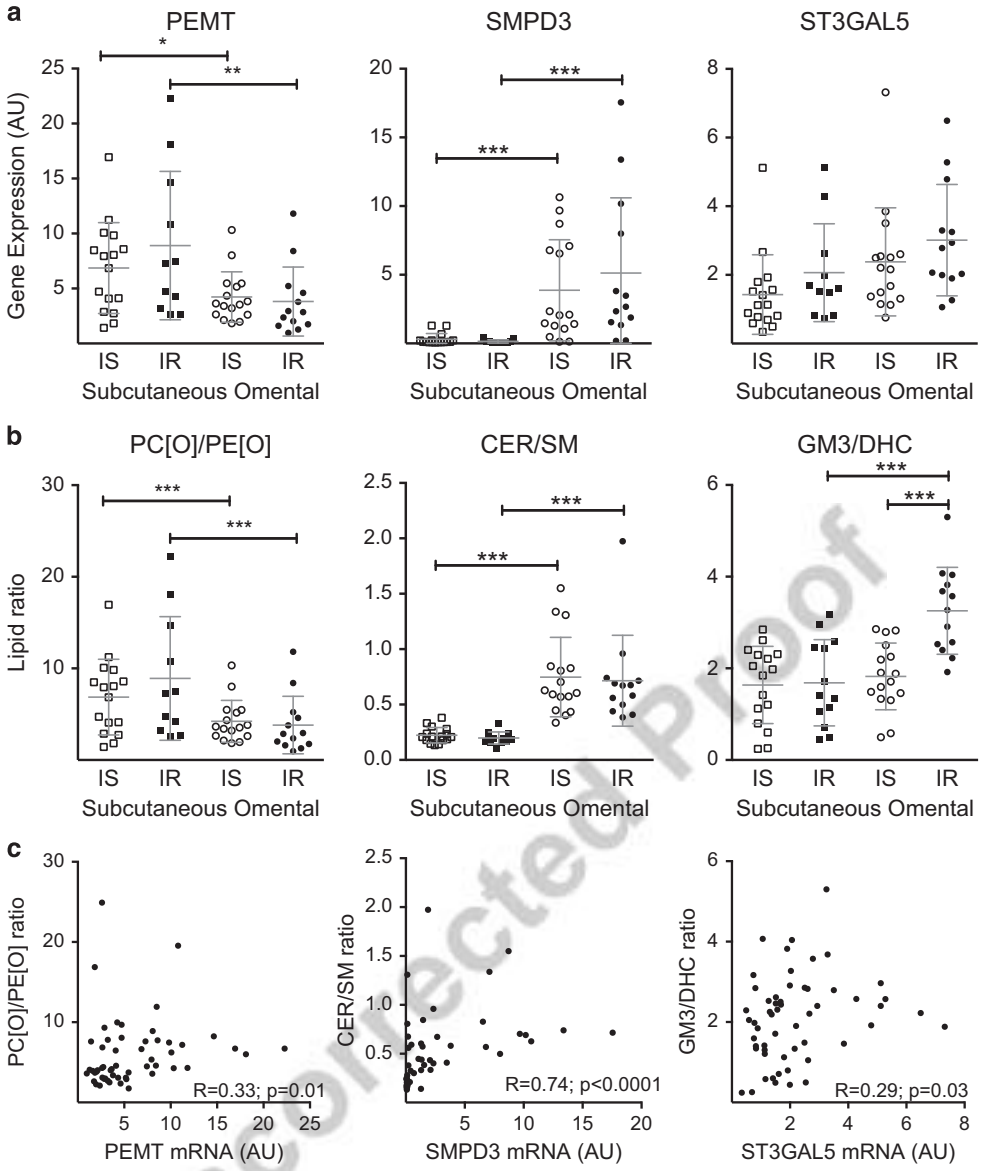

Figure 3. Differential expression of lipid metabolism genes correlates with lipid profiles of subcutaneous and omental adipose tissue. (**a**) Expression of *PEMT*, *SMPD3* and *ST3GAL5* relative to beta actin (*ACTB*). (**b**) Product/substrate ratios for each of these enzymes, according to subject group and adipose tissue depot. (**c**) Correlations between gene expression and lipid product/substrate ratios in all adipose tissue samples. AU: arbitrary units; *, ** and ***$P < 0.05$, 0.01 and 0.001 by *t*-test, respectively. mRNA from two IR subcutaneous adipose tissue samples was not available for these analyses. PC[O], PE[O], CER, SM, GM3 and DHC: alkylphosphatidylcholine, alkylphosphatidylethanolamine, ceramide, sphingomyelin, G_{M3} ganglioside and dihexosylceramide, respectively.

CONFLICT OF INTEREST

The authors declare no conflict of interest.

ACKNOWLEDGEMENTS

We are grateful to the women who participated in this study. The study was supported by a Diabetes Australia Research Trust (DART) Award, the Victorian State Government Operational Infrastructure Support and the Australian Government NHMRC IRIISS. JMW takes full responsibility for the work as a whole, including the study design, access to data and the decision to submit and publish the manuscript.

AUTHOR CONTRIBUTIONS

This study was designed by JMW, LCH, PEO and PM. JMW, GN, KN, CB, JW and MC performed the experiments. GKS and RL analysed the microarray data. JMW collated and analysed the results and drafted the manuscript. All authors edited the manuscript and approved it for submission.

REFERENCES

1 Garg A. Regional adiposity and insulin resistance. *J Clin Endocrinol Metab* 2004; **89**: 4206–4210.
2 Kotronen A, Yki-Jarvinen H, Sevastianova K, Bergholm R, Hakkarainen A, Pietilainen KH *et al.* Comparison of the relative contributions of intra-abdominal and liver fat to components of the metabolic syndrome. *Obesity (Silver Spring)* 2011; **19**: 23–28.
3 Defronzo RA. Banting lecture from the triumvirate to the ominous octet: a new paradigm for the treatment of type 2 diabetes mellitus. *Diabetes* 2009; **58**: 773–795.
4 Glass CK, Olefsky JM. Inflammation and lipid signaling in the etiology of insulin resistance. *Cell Metab* 2012; **15**: 635–645.
5 Turer AT, Scherer PE. Adiponectin: mechanistic insights and clinical implications. *Diabetologia* 2012; **55**: 2319–2326.
6 Stolic M, Russell A, Hutley L, Fielding G, Hay J, MacDonald G *et al.* Glucose uptake and insulin action in human adipose tissue—influence of BMI, anatomical depot and body fat distribution. *Int J Obes Relat Metab Disord* 2002; **26**: 17–23.
7 Kloting N, Fasshauer M, Dietrich A, Kovacs P, Schon MR, Kern M *et al.* Insulin-sensitive obesity. *Am J Physiol Endocrinol Metab* 2010; **299**: E506–E515.

8 Yang YK, Chen M, Clements RH, Abrams GA, Aprahamian CJ, Harmon CM. Human mesenteric adipose tissue plays unique role versus subcutaneous and omental fat in obesity related diabetes. *Cell Physiol Biochem* 2008; **22**: 531–538.
9 Hajri T, Tao H, Wattacheril J, Marks-Shulman P, Abumrad NN. Regulation of adiponectin production by insulin: interactions with tumor necrosis factor-alpha and interleukin-6. *Am J Physiol Endocrinol Metab* 2011; **300**: E350–E360.
10 Esser N, L'Homme L, De Roover A, Kohnen L, Scheen AJ, Moutschen M *et al.* Obesity phenotype is related to NLRP3 inflammasome activity and immunological profile of visceral adipose tissue. *Diabetologia* 2013; **56**: 2487–2497.
11 Kolak M, Westerbacka J, Velagapudi VR, Wagsater D, Yetukuri L, Makkonen J *et al.* Adipose tissue inflammation and increased ceramide content characterize subjects with high liver fat content independent of obesity. *Diabetes* 2007; **56**: 1960–1968.
12 Roberts R, Hodson L, Dennis AL, Neville MJ, Humphreys SM, Harnden KE *et al.* Markers of *de novo* lipogenesis in adipose tissue: associations with small adipocytes and insulin sensitivity in humans. *Diabetologia* 2009; **52**: 882–890.
13 Schaeffler A, Gross P, Buettner R, Bollheimer C, Buechler C, Neumeier M *et al.* Fatty acid-induced induction of Toll-like receptor-4/nuclear factor-kappaB pathway in adipocytes links nutritional signalling with innate immunity. *Immunology* 2009; **126**: 233–245.
14 Wen H, Gris D, Lei Y, Jha S, Zhang L, Huang MT *et al.* Fatty acid-induced NLRP3-ASC inflammasome activation interferes with insulin signaling. *Nat Immunol* 2011; **12**: 408–415.
15 Lipina C, Hundal HS. Sphingolipids: agents provocateurs in the pathogenesis of insulin resistance. *Diabetologia* 2011; **54**: 1596–1607.
16 Kabayama K, Sato T, Saito K, Loberto N, Prinetti A, Sonnino S *et al.* Dissociation of the insulin receptor and caveolin-1 complex by ganglioside GM3 in the state of insulin resistance. *Proc Natl Acad Sci USA* 2007; **104**: 13678–13683.
17 Ussher JR, Koves TR, Cadete VJ, Zhang L, Jaswal JS, Swyrd SJ *et al.* Inhibition of *de novo* ceramide synthesis reverses diet-induced insulin resistance and enhances whole-body oxygen consumption. *Diabetes* 2010; **59**: 2453–2464.
18 Aerts JM, Ottenhoff R, Powlson AS, Grefhorst A, van Eijk M, Dubbelhuis PF *et al.* Pharmacological inhibition of glucosylceramide synthase enhances insulin sensitivity. *Diabetes* 2007; **56**: 1341–1349.
19 Zhao H, Przybylska M, Wu IH, Zhang J, Siegel C, Komarnitsky S *et al.* Inhibiting glycosphingolipid synthesis improves glycemic control and insulin sensitivity in animal models of type 2 diabetes. *Diabetes* 2007; **56**: 1210–1218.
20 Kotronen A, Seppanen-Laakso T, Westerbacka J, Kiviluoto T, Arola J, Ruskeepaa AL *et al.* Comparison of lipid and fatty acid composition of the liver, subcutaneous and intra-abdominal adipose tissue, and serum. *Obesity (Silver Spring)* 2010; **18**: 937–944.
21 Jove M, Moreno-Navarrete JM, Pamplona R, Ricart W, Portero-Otin M, Manuel Fernandez-Real J. Human omental and subcutaneous adipose tissue exhibit specific lipidomic signatures. *FASEB J* 2013; **28**: 1071–1081.
22 Weir JM, Wong G, Barlow CK, Greeve MA, Kowalczyk A, Almasy L *et al.* Plasma lipid profiling in a large population-based cohort. *J Lipid Res* 2013; **54**: 2898–2908.
23 Shi W, Oshlack A, Smyth GK. Optimizing the noise versus bias trade-off for Illumina whole genome expression BeadChips. *Nucleic Acids Res* 2010; **38**: e204.
Q11 24 Smyth GK. Linear models and empirical bayes methods for assessing differential expression in microarray experiments. *Stat Appl Genet Mol Biol* 2004; **3**.
25 Wentworth JM, Naselli G, Brown WA, Doyle L, Phipson B, Smyth GK *et al.* Pro-inflammatory CD11c+CD206+ adipose tissue macrophages are associated with insulin resistance in human obesity. *Diabetes* 2010; **59**: 1648–1656.
26 Xu H, Barnes GT, Yang Q, Tan G, Yang D, Chou CJ *et al.* Chronic inflammation in fat plays a crucial role in the development of obesity-related insulin resistance. *J Clin Invest* 2003; **112**: 1821–1830.
27 Ashburner M, Ball CA, Blake JA, Botstein D, Butler H, Cherry JM *et al.* Gene ontology: tool for the unification of biology. The Gene Ontology Consortium. *Nat Genet* 2000; **25**: 25–29.
28 Tanabe M, Kanehisa M. Using the KEGG database resource. *Curr Protoc Bioinformatics* 2012. Q12
29 Cancello R, Tordjman J, Poitou C, Guilhem G, Bouillot JL, Hugol D *et al.* Increased infiltration of macrophages in omental adipose tissue is associated with marked hepatic lesions in morbid human obesity. *Diabetes* 2006; **55**: 1554–1561.
30 Yamashita T, Hashiramoto A, Haluzik M, Mizukami H, Beck S, Norton A *et al.* Enhanced insulin sensitivity in mice lacking ganglioside GM3. *Proc Natl Acad Sci USA* 2003; **100**: 3445–3449.
31 Tagami S, Inokuchi Ji J, Kabayama K, Yoshimura H, Kitamura F, Uemura S *et al.* Ganglioside GM3 participates in the pathological conditions of insulin resistance. *J Biol Chem* 2002; **277**: 3085–3092.
32 Shungin D, Winkler TW, Croteau-Chonka DC, Ferreira T, Locke AE, Magi R *et al.* New genetic loci link adipose and insulin biology to body fat distribution. *Nature* 2015; **518**: 187–196.
33 Vohl MC, Sladek R, Robitaille J, Gurd S, Marceau P, Richard D *et al.* A survey of genes differentially expressed in subcutaneous and visceral adipose tissue in men. *Obes Res* 2004; **12**: 1217–1222.
34 Klimcakova E, Roussel B, Marquez-Quinones A, Kovacova Z, Kovacikova M, Combes M *et al.* Worsening of obesity and metabolic status yields similar molecular adaptations in human subcutaneous and visceral adipose tissue: decreased metabolism and increased immune response. *J Clin Endocrinol Metab* 2011; **96**: E73–E82.
35 Horl G, Wagner A, Cole LK, Malli R, Reicher H, Kotzbeck P *et al.* Sequential synthesis and methylation of phosphatidylethanolamine promote lipid droplet biosynthesis and stability in tissue culture and in vivo. *J Biol Chem* 2011; **286**: 17338–17350.
36 Cinti S, Mitchell G, Barbatelli G, Murano I, Ceresi E, Faloia E *et al.* Adipocyte death defines macrophage localization and function in adipose tissue of obese mice and humans. *J Lipid Res* 2005; **46**: 2347–2355.
37 Kolak M, Gertow J, Westerbacka J, Summers SA, Liska J, Franco-Cereceda A *et al.* Expression of ceramide-metabolising enzymes in subcutaneous and intra-abdominal human adipose tissue. *Lipids Health Dis* 2012; **11**: 115.
38 Kotronen A, Velagapudi VR, Yetukuri L, Westerbacka J, Bergholm R, Ekroos K *et al.* Serum saturated fatty acids containing triacylglycerols are better markers of insulin resistance than total serum triacylglycerol concentrations. *Diabetologia* 2009; **52**: 684–690.
39 Haus JM, Kashyap SR, Kasumov T, Zhang R, Kelly KR, Defronzo RA *et al.* Plasma ceramides are elevated in obese subjects with type 2 diabetes and correlate with the severity of insulin resistance. *Diabetes* 2009; **58**: 337–343.
40 Meikle PJ, Wong G, Barlow CK, Weir JM, Greeve MA, MacIntosh GL *et al.* Plasma lipid profiling shows similar associations with prediabetes and type 2 diabetes. *PLoS One* 2013; **8**: e74341.
41 Wong G, Barlow CK, Weir JM, Jowett JB, Magliano DJ, Zimmet P *et al.* Inclusion of plasma lipid species improves classification of individuals at risk of type 2 diabetes. *PLoS One* 2013; **8**: e76577.

Supplementary Information accompanies this paper on International Journal of Obesity website (http://www.nature.com/ijo)